

Ho activity would amount to about 40 disintegrations/minute. With a transmission of  $10^{-6}$  for the spectrometer, any contribution to the Er  $K$  x-rays from the Ho<sup>166</sup> activity that might be present would be negligible.

Since Graham *et al.*<sup>1</sup> set a 0.01% upper limit for positron emission, one is thus left with the fourth and final alternative; the Er  $K$  x-rays are due to a small  $K$ -capture branch in the Tm<sup>170</sup> decay. Taking the intensity of the Yb  $K$  x-rays as 0.094 per disintegration<sup>1</sup> and ignoring the  $K$  x-rays that might be coming from conversion on the  $K$ -capture side, the intensity of the  $K$ -capture branching ratio is calculated to be 0.15%. This value is consistent with that of Graham *et al.*,<sup>1</sup> who set an upper limit of 0.3%.

With the establishment of the  $K$ -capture branch, it seemed worthwhile to look for the presence of a gamma ray associated with the de-excitation of the first rotational level in Er<sup>170</sup>. From a plot of the energy of the first excited state of the even-even nuclei as a function of mass number, one would estimate that the energy of the first excited state of Er<sup>170</sup> would lie somewhere in the region between seventy and eighty-

five kev. If the  $K$ -branch proceeded entirely through the first excited state, one would expect the intensity of the gamma ray (no conversion) to be about 5% of the 84-kev gamma ray. With the present resolution of about 1.8% in this region and only a moderately intense source (84-kev gamma peak counting rate of 400 counts/min), it would be difficult to see a 5% contribution to the 84-kev gamma ray from the Er<sup>170</sup> gamma ray in the region between 82.7 and 85.7 kev. A search was made on the bent-crystal spectrometer in the 70- to 83-kev region and the 85- to 90-kev region; there was no evidence of any gamma ray present with an intensity greater than 2% of the 84-kev gamma ray. However, systematics indicate that the gamma rays would have about the same conversion coefficients and that the branching ratios to the first excited level in each daughter nucleus would be about the same ( $\approx 20\%$ ), and thus the Er  $K$  x-rays arise mainly in the  $K$ -capture process rather than in  $K$  conversion. Thus the ratio of the two gamma-ray intensities should be about  $2 \times 10^{-3}$ . Therefore it is not surprising that this line was not observed.

## Neutron Resonances in the kev Region\*

JOHN H. GIBBONS†

*Department of Physics, Duke University, Durham, North Carolina*

(Received August 11, 1954; revised manuscript received February 13, 1956)

A neutron collimation-detection system has been constructed for use in measurements of resonance neutron cross sections. The high efficiency of the detector in combination with careful collimator design enables one to collect data with relatively good resolution in a short time. Although designed to measure cross sections at a minimum energy of about 5 kev, resonances have been observed at energies as low as 350 ev. Resolving power exceeds that of velocity selectors, however, only at neutron energies greater than about 5 kev. Resonances in iron were found at 8, 29, 75, and 85 kev. The three latter resonances exhibit strong interference dips and are assumed to be due to  $s$ -wave neutrons on Fe<sup>56</sup>. The resonance energies found in bismuth were 1, 3, 13, 16, 34, 47, and 70 kev; the level spacing for a single  $J$  value thus seems to be about 20 kev.

### INTRODUCTION

THERE is now considerable evidence<sup>1-7</sup> that the effects of magic neutron numbers on nuclear level density are evident even at excitation energies of 5-8 Mev. One of the most direct methods of investi-

gation of this effect is the study of neutron total cross sections in the resonance region. Many "magic" or "near-magic" nuclei have resonance spacings of the order of 1 to 10 kev. With a spectrometer of 5 to 10% resolving power in the range 5 to 100 kev one could also hope to finish bridging the gap<sup>8</sup> between neutron cross sections obtained by velocity selectors (0-5 kev) and the other principle group of data, whose low-energy side is somewhat below 100 kev. Finally, determination of resonance parameters, such as reaction width and spin of many levels previously too narrow to measure, should be feasible.

This paper reports the successful construction of a

\* This work was supported by the U. S. Atomic Energy Commission.

† Now at Oak Ridge National Laboratory, Oak Ridge, Tennessee.

<sup>1</sup> Hughes, Spatz, and Goldstein, *Phys. Rev.* **75**, 1781 (1949).

<sup>2</sup> D. J. Hughes and D. Sherman, *Phys. Rev.* **78**, 632 (1950).

<sup>3</sup> J. H. Gibbons and H. W. Newson, *Phys. Rev.* **91**, 209(A) (1953).

<sup>4</sup> H. W. Newson and R. H. Rohrer, *Phys. Rev.* **94**, 654 (1954); **87**, 177 (1952).

<sup>5</sup> Miller, Adair, Bockelman, and Darden, *Phys. Rev.* **88**, 83 (1952).

<sup>6</sup> Hughes, Garth, and Levin, *Phys. Rev.* **91**, 1423 (1953).

<sup>7</sup> Harvey, Hughes, Carter, and Pilcher, *Phys. Rev.* **99**, 10 (1955).

<sup>8</sup> D. J. Hughes and J. A. Harvey, *Neutron Cross Sections*, Brookhaven National Laboratory Report BNL-325 (Superintendent of Documents, U. S. Government Printing Office, Washington, D. C., 1952).

spectrometer fitted to the foregoing specifications and includes some early results. The design is along very similar lines to the spectrometer of Langsdorf *et al.*<sup>9,10</sup> and has the added feature of high neutron efficiency, so that a large amount of data can be taken in a relatively short time.

#### APPARATUS

The proton beam from the Duke Van de Graaff accelerator was both magnetically and electrostatically analyzed to a resolution of about 0.07% before impinging upon a thin (<1 kev) Li target evaporated onto a thin metal backing. Analyzed beam currents of 5 to 10 microamperes were used. Neutrons from the  $\text{Li}^7(p,n)$  reaction, emerging at an angle of  $122^\circ$  measured from the direction of the incident protons, were collimated over a distance of about four feet (Fig. 1) by means of paraffin and water shielding. The angular spread of the accepted neutron beam was  $2^\circ$  in the plane of the figure and  $20^\circ$  in the plane normal to the page. These values were chosen as a compromise between resolution and expected counting rates. The calculated resolution of the collimation system is shown in Fig. 2; the additional energy spreads in the experiment (due to finite proton beam resolution and target thickness) were omitted in the above calculation.

The neutron detection system (labeled the "Box") consisted of a bank of 18 high-pressure (120 cm)  $\text{B}^{10}\text{F}_3$  proportional counters<sup>11</sup> connected in parallel and embedded in a paraffin matrix<sup>12</sup> (Fig. 1). These counters had a 20-inch active length. The radial spacing of the counters (2 in. center-to-center) was chosen for 75% "thermal utilization."

The decision to use a  $\text{B}^{10}\text{F}_3$  pressure of 120 cm Hg was based on a relative efficiency test using identical geometry with gas pressures ranging from 100 to 150 cm Hg. Pressures lower than 120 cm Hg produced more uniform pulses but lower efficiency. Higher pressures resulted in poorer  $\gamma$ -ray discrimination, giving an effective decrease in efficiency. The number of neutron events biased out (in order to avoid any counts from  $\gamma$  rays) was estimated to be about 18% of the total events in the counter. Spurious counts, due mainly to high-voltage leakage pulses, were eliminated by careful cleaning of components with ether and by maintaining these components at a slightly elevated temperature to reduce the relative humidity of the surrounding air.

The neutron monitor, placed at  $0^\circ$  with respect to the proton beam, consisted of a single  $\text{BF}_3$  counter embedded along the axis of a cadmium-covered paraffin cylinder, 6 in. in diameter and 2 ft long. The front face of the cylinder was perforated with six 1-in. diameter

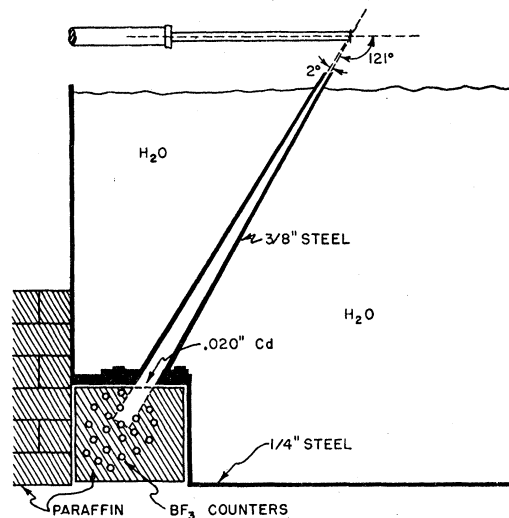


FIG. 1. A cross-sectional view of the experimental arrangement. Center-to-center spacing of  $\text{BF}_3$  counters is 2 in.

holes drilled 8 in. deep (similar to the design of a McKibben counter) in order to improve the counter's linearity and efficiency.

#### TARGETS

Lithium metal was evaporated in vacuum on 0.005-in. tantalum caps, of 1-in. outer diameter, with a  $\frac{1}{8}$ -in. lip for sealing (with a plastic cement) to the Van de Graaff vacuum system (more recent methods are

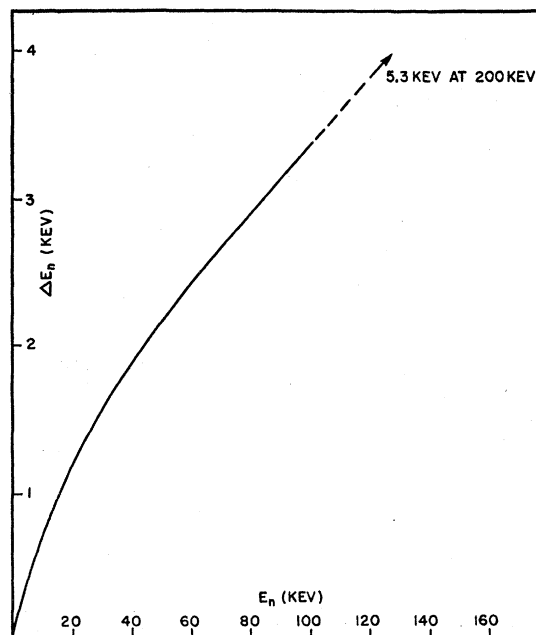


FIG. 2. Calculated resolution of collimator. Effects of proton energy spread and lithium target thickness have been omitted. A method of exact determination of the energy spread due to the latter effects is under study.

<sup>9</sup> A. L. Langsdorf, Jr., Phys. Rev. **80**, 132 (1950).

<sup>10</sup> Hibdon, Langsdorf, and Holland, Phys. Rev. **85**, 595 (1952).

<sup>11</sup> Made by special order by Radiation Counter Laboratories, Skokie, Illinois. A glass filling system was used.

<sup>12</sup> P. R. Bell, unpublished curve of thermal neutron intensity as a function of distance in water, using an Sb-Be neutron source.

discussed in the sections on Background and Later Improvements). These were stored in an evacuated desiccator until used. The targets were exposed to air for a total of less than one minute. Selection for use was based on relative neutron yield and resolution as determined by the measured transmission at the 13-keV bismuth resonance. A Bi sample 1 cm thick was used. Targets were discarded if  $T_{\min}$  was greater than 60%. The lowest transmission value measured was 47% but the average value was about 52%. Targets were also discarded at times because of poor reproducibility in counting. This effect seems to be due to a nonuniform lithium layer.<sup>13</sup> The target was cooled by a fine air-water spray. Counting rates ranged from  $\sim 5 \times 10^2$  cpm at  $E_n = 500$  ev to  $\sim 10^4$  cps at  $E_n = 50$  kev for proton beam currents of about 6  $\mu$ a. Naturally these values changed from target to target, but never more than a factor of two in either direction.

### PROCEDURE

Alignment (other than visual) of all components was accomplished by maximizing proton current or neutron counting rate. Normalization of counts was obtained by proton current integration and by monitoring the neutron counting rate at  $0^\circ$ . About 5000 counts were usually taken.

Energy calibration of the electrostatic analyzer voltage was obtained by measuring the forward threshold of the  $\text{Li}^7(p,n)$  reaction. The extrapolation (to zero counting rate) of the linear portion of the forward yield curve was assumed to correspond to a proton energy of 1.882 Mev. This point, however, refers to the energy of the high-energy portion of the proton beam distribution function. The energy of the peak of the distribution function is slightly ( $\leq 0.5$  kev) less than this. For a proton energy error of 0.5 kev, the

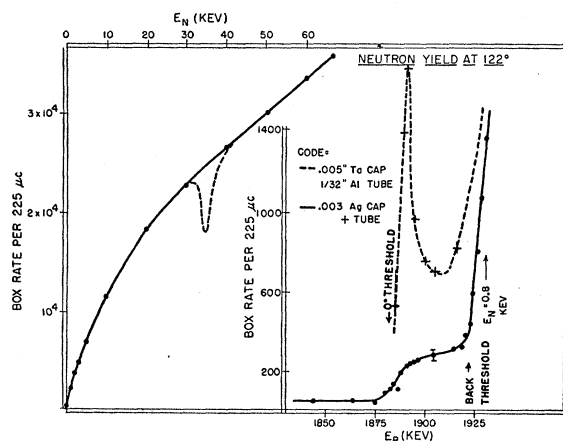


FIG. 3. Relative neutron yield at  $122^\circ$ . The right side of the figure is an enlargement (and extension to lower proton energy) of the yield curve on the left. The two curves nearly coincide above 1 kev.

<sup>13</sup> A. L. Langsdorf, Jr. (private communication).

corresponding neutron energy error (at  $122^\circ$ ) is about 0.25 kev for  $E_n > 20$  kev and decreases with decreasing energy, becoming about 100 ev at  $E_n = 2$  kev. Attempts to determine the exact energy of the peak of the proton distribution are hindered by several factors: (1) uncertainties in the proton distribution curve as to both width and shape; (2) target thickness uncertainty. These factors are under study, but it has been decided, for the present, to report our cross section measurements with the usual energy assignment, i.e., without correction for the error mentioned above. Hence, we quote a neutron energy uncertainty of  $\pm 0.5$  kev,  $-0.25$  kev for  $E_n < 10$  kev. During preliminary runs, when only the magnetic analyzer was in use, energy calibration was performed by measuring the relative magnetic field corresponding to several known neutron resonances. Calibration of neutron energies in later runs was determined from the measured proton energy.

### BACKGROUNDS

With the exception of a small cosmic-ray component, background was limited to neutrons that entered the detector via the collimator. A paraffin scatterer, shaped like the collimator, was inserted between the top of the collimator and the target. The thickness of the paraffin corresponded to about 30 mean free paths of a 10-kev neutron. Table I summarizes the results obtained.

The data in the third column indicate the presence of neutrons entering through the collimator even though all neutrons produced by the  $\text{Li}^7(p,n)$  reaction should, at this proton energy, be found only in a forward angle cone. This counting rate was found to be due to neutron back-scattering by the target backing. A typical yield curve near threshold is shown on the right side of Fig. 3. The dotted curve resulted from a target arrangement consisting of aluminum vacuum tubing with tantalum target backing. The peak shown at  $E_p = 1890$  kev is due to neutrons produced in the Li target, then back-scattered by the tantalum, and finally *resonantly* scattered by the 37-kev resonance in the aluminum tube. A similar process due to the 90-kev aluminum resonance was probably responsible for the rise in counting rate slightly below  $E_p = 1922$  kev (threshold for neutrons into back angles).

Since this background of off-energy neutrons reduces the apparent cross section of resonance peaks, the

TABLE I. Counting rates at  $122^\circ$  in the vicinity of the  $\text{Li}^7(p,n)$  threshold.

	Machine off	$E_p < E_{th}(0^\circ)$	$E_{th}(122^\circ)$ $> E_p > E_{th}(0^\circ)$	$E_p > E_{th}(122^\circ)$
Counting rate (cpm), no paraffin absorbers	20±2	22±2	87±9	2000
Counting rate, with paraffin absorbers	no data	no data	15±6	21±2

following changes were introduced in an attempt to reduce the magnitude of the background.

(1) The 0.005-in. thick Ta target backing was replaced by 0.003-in. Ag.

(2) In order to eliminate irregularities in the neutron yield curve at  $122^\circ$  as well as to determine the magnitude of the back-scattered neutrons near back threshold, the  $\frac{1}{2}$ -in. wall, 1 in. o.d. aluminum vacuum tubing was replaced by a 0.010-in. wall,  $\frac{3}{4}$  in. o.d. silver tube. The resonance spacing in Ag is quite close, thus, for our resolving power, neutrons passing through the Ag tube "see" a constant cross section rather than a variable one as was the case for Al.

The data for the solid curves shown in Fig. 3 were taken after the preceding changes were effected. The improvement attained is quite evident. Previously, for instance, a prominent dip (see Fig. 3) in the yield curve appeared near 37 keV.

#### CORRECTIONS TO THE DATA

As mentioned in the previous section, backgrounds were of two types: (1) cosmic-ray neutrons; (2) neutrons back-scattered by the target backing.

The correction for (1) becomes less than 1% for neutron energies  $>5$  keV but was usually applied to data below this energy.

An approximate correction factor can be made for background (2) since it is due to neutrons interacting with the sample with a cross section roughly equal to the average cross section of the sample in the energy region under study. This is because the energy spread of the scattered neutron group ranges (more or less uniformly) from the energy of the direct beam (at  $122^\circ$ ) to an energy some 120 keV greater, corresponding to neutrons whose original direction was  $0^\circ$ . When the energy of the direct neutron beam is such that the sample exhibits only potential scattering, very little correction is ordinarily needed for the off-energy scattered group. But when the energy of the direct beam corresponds to a resonance in the sample, a much larger correction may be made for the presence of the off-energy group provided the relative magnitude of the two groups is known.

The counting rate slightly below  $122^\circ$  threshold is a measure of this effect, but since the neutron flux from the  $\text{Li}^7(p,n)$  reaction has a strong energy-angle dependence, and since the amount of target backing "seen" by neutrons is also dependent upon angle, the flux of back-scattered neutrons at  $122^\circ$  may very well change with proton energy.

An accurate calculation of this effect was attempted, but it was soon found more feasible to measure the background with the aid of elements with strong, isolated resonances. Those chosen were the 3-keV sodium and the 37-keV aluminum resonances. The effective cross section at resonance was measured for

several values of sample thickness. After correction<sup>14</sup> for finite energy resolution of the direct beam and for nonexponential beam attenuation due to thick samples, one is able to estimate to within several percent the fraction of the total beam attributable to the scattered, off-energy group. The results showed that the absolute rate of scattered neutrons does not change between back threshold and  $E_n(122^\circ)=3$  keV, but seems to increase slightly by 37 keV. This correction has been applied to very few curves thus far since its only effect is to accentuate a resonance already found. A closer study of the correction is now underway in this laboratory.

A check was made to determine whether in-scattering corrections might be needed when large samples were used. As expected (from the long collimation path), tests showed that in-scattering corrections were negligible.

#### EXPERIMENTAL RESULTS

The results below serve to indicate the ability of the spectrometer to measure total cross sections at relatively high resolution. Data taking time for the iron curve, for instance, was about 10 hours.

##### Iron

The total cross section of iron is shown in Fig. 4. This curve was calculated from the raw data with no corrections applied. The sample was 3.24 g/cm<sup>2</sup> wrought iron. The resonances at 28.8, 74.5, and 84.5 keV seem to be due to s-wave ( $l=0$ ) neutrons interacting with  $\text{Fe}^{56}$ . The resonance at 28.8 keV has been observed by others,<sup>15</sup> and the peak previously reported at 90 keV may be an average of the pair we found at 74.5 and 84.5 keV. The other definite resonance observed (at 8.0 keV) confirms the work of Hibdon *et al.*<sup>10</sup> We too found slight evidence for a very weak resonance near 16 keV and another near 36 keV. These resonances and the one at 8.0 keV are due either to resonances in a minor isotope or to resonances in  $\text{Fe}^{56}$  of neutrons with  $l>0$ . This problem should be readily solvable by measuring the cross sections of iron enriched in the minor isotopes. We plan to do this in the near future.

Since the neutron collimator was constructed of iron, one might think that at certain neutron energies the collimator could scatter or transmit a large number of neutrons, thus seriously affecting the operation of the spectrometer. Fortunately, this is not true. For a cross section as low as 0.5 barn, the collimator walls still reduce the neutron transmission to about 1%. Perhaps the best answer concerning possible bad effects in high cross-section regions is that, although a great variety of elements and sample sizes have been run

<sup>14</sup> E. Merzbacher (unpublished). The method used was similar to that mentioned in B. T. Feld *et al.*, Atomic Energy Commission Report, NYO 636, TS1, Oak Ridge, 1951 (unpublished), p. 33 ff.

<sup>15</sup> Barschall, Bockelman, and Seagondollar, Phys. Rev. **73**, 659 (1948).

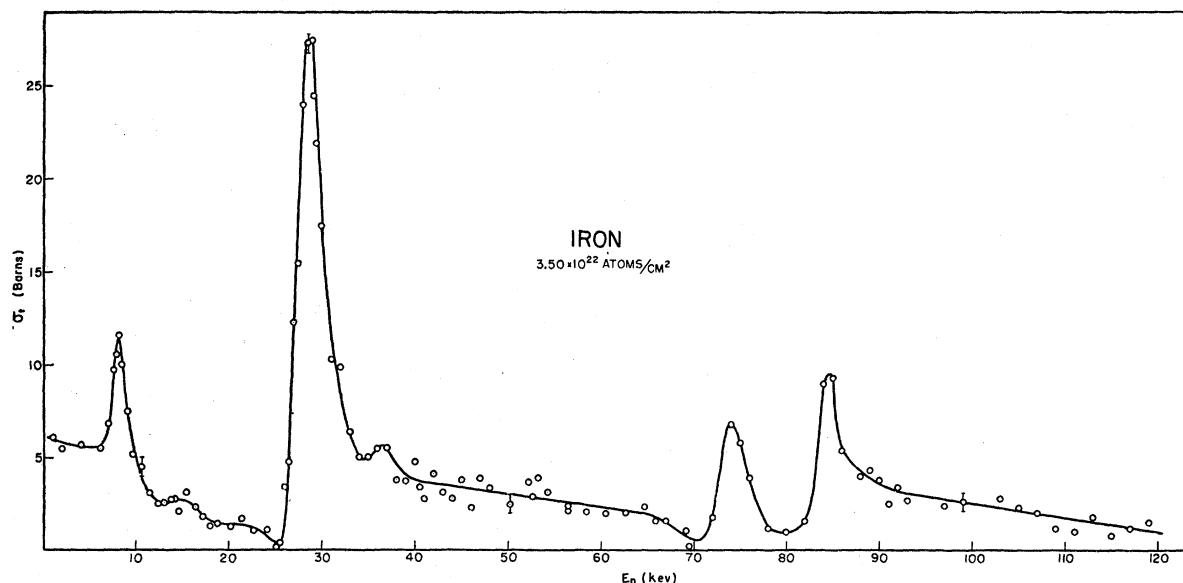


FIG. 4. Total cross section of iron. Probable errors of all points are about the same as those indicated. Resolving power at 30 keV is 2 keV.

using this apparatus, no consistent effect seems to occur that might indicate trouble arising from using iron as a collimator.

#### Rubidium

Figure 5 shows a resonance measured in a sample of rubidium chloride. The curve represents the original data with no corrections. The sample was pressed from a finely divided powder form into a rectangular block and sealed in 0.001 in. silver foil. Instead of taking the usual "in" and "out" measurements, the "out" measure-

ment in this case was the neutron beam transmitted through a rectangular block of  $C_2Cl_6$  (also sealed in 0.001 in. silver foil) which contained an areal density of chlorine equal to that in the  $RbCl$  sample. Thus the ratio in/out canceled out all terms except rubidium and carbon. A carbon correction was then made, assuming  $\sigma_T(C) = \text{constant} = 4.6$  barns. This procedure works well except in the neighborhood of a strong resonance; natural chlorine has only one such resonance at about 27 keV. More complete reports on the cross section of rubidium and its isotopes will appear later. This presentation simply serves to indicate the spectrometer's resolving power near 5-keV neutron energy.

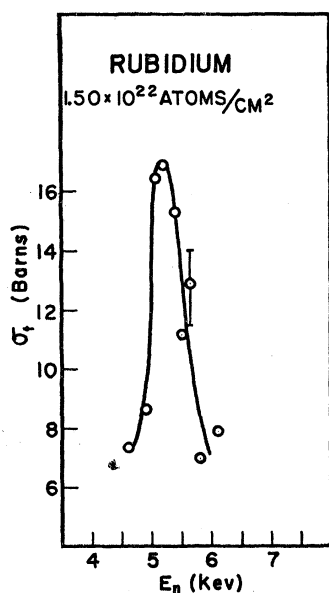


FIG. 5. A resonance in the cross section of rubidium.

#### Manganese and Zinc

At very low neutron energies the contributions from all three sources of finite energy resolution (proton energy spread, target thickness, and collimator acceptance angle) approach zero because of the small slope of the curve relating  $E_n(122^\circ)$  and  $E_p$ . Unfortunately, the neutron yield also approaches zero; but if one is willing to endure long counting times, he should be able to observe resonances spaced only a few hundred electron volts apart. Figure 6 shows that this is indeed the case.

The curves have had no correction applied and are plotted as *transmission versus* proton energy. Corrections for neutrons scattered in the target backing are quite large in this region ( $\sim 50\%$ ) and hence must be determined more accurately before they (the corrections) are sufficiently trustworthy to report. Neutron energies at resonance (minima in the trans-

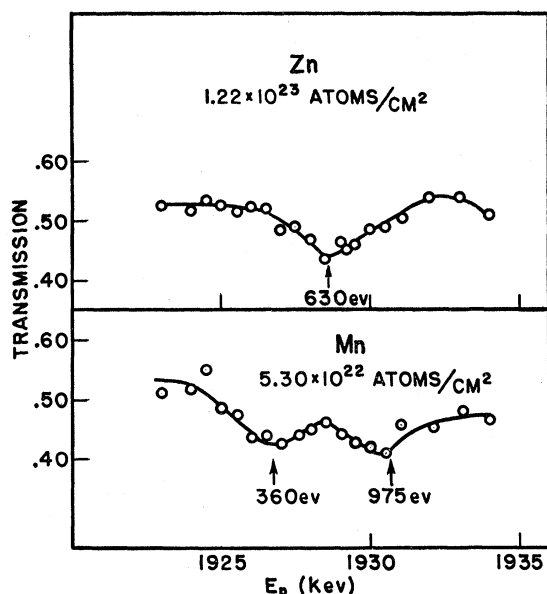


FIG. 6. Neutron transmission curves of manganese and zinc. This is the lowest energy region examined with this equipment.

mission curves) are indicated. These two curves were taken concurrently.

These measurements confirm the work of others<sup>8</sup> well within our energy uncertainty. These results are not meant to imply that it is feasible for us to make extensive measurements in this region. They serve only to demonstrate the versatility of the spectrometer.

### Bismuth

The results for bismuth are seen in Fig. 7. All essential features have been measured at least twice. All background corrections have been applied. The effect of the corrections, for example, on the 13-kev resonance was to increase the apparent peak cross section from 27 to 31 barns. The resonances shown at about 1 and 3 kev are undoubtedly the ones reported at 0.8 and 2.5 kev by the Argonne fast chopper group.<sup>8</sup> Typically shaped *s*-resonances appear at 3, 13, 34, 47, and 70 kev. The Argonne data have shown that the 1-kev resonance is also due to *s*-neutrons.

The point scatter around 6 kev has been checked and no evidence was found indicating real structure. Thus the level spacing for single spin and parity seems to be on the order of 20 kev, assuming a random distribution of spin states.

### LATER IMPROVEMENTS

One of the primary difficulties encountered in these measurements was the relatively short, useful lifetime

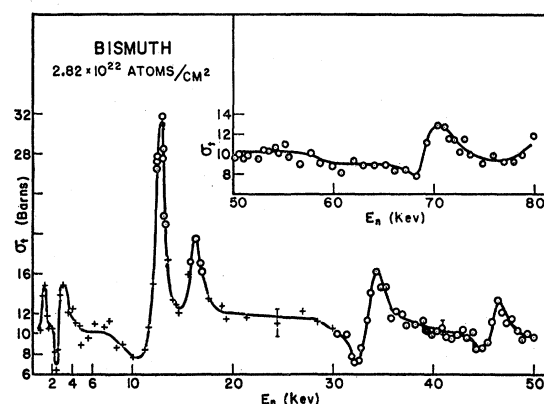


FIG. 7. Total cross section of bismuth. Crosses and circles represent two independent runs. Probable errors of all points are about the same as those indicated.

of targets (about 16 hours). During this time a thin but apparently uneven deposit of carbon was built up on the lithium surface. Although frequent measurements of the  $\text{Li}(p,n)$  threshold were made to correct energy shifts, this condition was obviously unsatisfactory, since the uneven carbon build-up worsened the resolution. We have been able to improve the useful lifetime by a factor of at least ten by introducing the following changes and modifications:

- (1) The 0.003 in. silver target backings were found to be unsatisfactory due to "blister" formation on the lithium coated surface in the immediate area bombarded by the protons. The substitution of platinum for silver seems to have eliminated this problem and also allowed us to reduce the target backing to 0.002 in. thick.
- (2) All glue and Neoprene "O" rings were removed from the target area. This was accomplished by using solder seals and lead "O" rings.
- (3) A liquid air-charcoal trap was installed within 3 in. of the target. This improved the vacuum at the target from  $4 \times 10^{-5}$  to  $2 \times 10^{-6}$  mm mercury and caused an order-of-magnitude decrease in carbon build-up rate. When the trap was moved 6 in. from the target, the build-up rate increased noticeably.

### ACKNOWLEDGMENTS

The author is greatly indebted to Dr. Henry W. Newson for suggesting this problem and for his invaluable assistance, advice, and encouragement. Valuable help was also given by members of the Duke Van de Graaff group, especially Dr. R. M. Williamson, Dr. H. Marshak, and Dr. R. Block. Helpful correspondence with Dr. A. Langsdorf of Argonne National Laboratory is gratefully acknowledged.